THE JOURNAL OF BIOLOGICAL CHEMISTRY VOL. 284, NO. 11, pp. 6955–6965, March 13, 2009

Atrophin Proteins Interact with the Fat1 Cadherin and Regulate Migration and Orientation in Vascular Smooth Muscle Cells*[S]

Received for publication, December 11, 2008 Published, JBC Papers in Press, January 7, 2009, DOI 10.1074/jbc.M809333200

Rong Hou and Nicholas E. S. Sibinga[1]

From the Department of Medicine, Cardiovascular Division, and Department of Developmental and Molecular Biology, Albert Einstein College of Medicine, Bronx, New York 10461

Fat1, an atypical cadherin induced robustly after arterial injury, has significant effects on mammalian vascular smooth muscle cell (VSMC) growth and migration. The related *Drosophila* protein Fat interacts genetically and physically with Atrophin, a protein essential for development and control of cell polarity. We hypothesized that interactions between Fat1 and mammalian Atrophin (Atr) proteins might contribute to Fat1 effects on VSMCs. Like Fat1, mammalian Atr expression increased after arterial injury and in VSMCs stimulated with growth and chemotactic factors including angiotensin II, basic fibroblast growth factor, and platelet-derived growth factor BB. Two distinct *Atr2* transcripts, *atr2L* and *atr2S,* were identified by Northern analysis; in VSMCs, *atr2S* mRNA expression was more responsive to stimuli. By immunocytochemistry, Fat1 and Atrs colocalized at cell-cell junctions, in the perinuclear area, and in the nucleus. In coimmunoprecipitation studies, Fat1 interacted with both Atr1 and Atr2; these interactions required Fat1 amino acids 4300–4400 and an intact Atro-box in the Atrs. Knockdown of Atrs by small interfering RNA did not affect VSMC growth but had complex effects on migration, which was impaired by Atr1 knockdown, enhanced by Atr2L knockdown, and unchanged when both Atr2S and Atr2L were depleted. Enhanced migration caused by Atr2L knockdown required Fat1 expression. Similarly, orientation of cells after monolayer denudation was impaired in cells with Atr1 knockdown but enhanced in cells selectively depleted of Atr2L. Together these findings suggest that Fat1 and Atrs act in concert after vascular injury but show further that distinct Atr isoforms have disparate effects on VSMC directional migration.

Migration and proliferation of VSMCs[2] in the wall of injured blood vessels are critical activities in the pathogenesis of atherosclerosis and related, clinically important vascular diseases. Arterial injury strongly induces expression of the Fat1 cadherin, which has distinct effects on VSMC migration and proliferation (1). Fat1 and related, atypical cadherins form a subfamily characterized by large extracellular domains containing 34 cadherin motifs, a variable number of EGF repeats, one or two laminin A/G domains, and a single transmembrane domain (2). In vertebrates, the Fat subfamily consists of four members, Fat1, -2, -3, and -4 (or Fat-J), whereas in *Drosophila*, two members, Fat and Fat-like, have been identified (2, 3). Although the *Drosophila fat* (*ft*) mutation, which causes enlargement of all larval imaginal discs, including wing, leg, eye-antenna, haltere, and genital imaginal discs, was first described by Mohr 85 years ago (4), understanding of how Fat proteins control developmental processes has only recently started to emerge.

Distinct functions have been ascribed to *Drosophila* Fat and Fat-like. The former acts as a suppressor of hyperplastic growth, as mentioned above, and as a mediator of planar cell polarity signals in development (4, 5). Fat has been identified in several recent studies as a regulator of the Hippo signaling pathway, which controls organ size during development through effects on both cell proliferation and survival (6–10). Fat-like, on the other hand, performs a crucial morphogenetic role in the formation of tubular organs such as the trachea, possibly by acting as an epithelial spacer (11). In contrast to the effect of Fat mutations, impairment of Fat-like expression does not affect imaginal disc development or planar cell polarity (11), but whether or not Fat and Fat-like have redundant or overlapping functions in other settings has not been fully explored.

Information about the function of vertebrate Fat proteins is relatively limited. Mice with homozygous inactivation of the *fat1* locus die perinatally with loss of the renal glomerular slit junctions, fusion of glomerular epithelial cell processes, and defects in forebrain and eye development; growth perturbations were not detected during embryonic skin development or in neurospheres derived from *fat1*$^{-/-}$ mice (12). In cultured cells, Fat1 interacts with Ena/VASP proteins, localizes to filopodial tips and lamellipodia at cellular leading edges, organizes cytoskeletal actin, and promotes migration (13, 14). We identified increased Fat1 expression in VSMCs responding to arterial injury and found that knockdown of Fat1 in this cell type limited migration but enhanced proliferation (1); taken together with the findings in *fat1*$^{-/-}$ mice (12), these results point to cell type- or developmental stage-dependent differences in the ability of Fat1 to regulate growth. Additional evidence for Fat1 function as a tumor suppressor includes the recent report of very frequent homozygous deletion or gene silencing of the *fat1* locus in oral squamous cell carcinomas (15). As for the other

* This work was supported, in whole or in part, by National Institutes of Health Grants HL67944 and CA086289 (to N. E. S. S.) and by American Heart Association Grant 0555803T. The costs of publication of this article were defrayed in part by the payment of page charges. This article must therefore be hereby marked "*advertisement*" in accordance with 18 U.S.C. Section 1734 solely to indicate this fact.

[S] The on-line version of this article (available at http://www.jbc.org) contains supplemental Figs. S1–S5.

[1] To whom correspondence should be addressed: Forchheimer G46, Albert Einstein College of Medicine, 1300 Morris Park Ave., Bronx, NY 10461-1602. Tel.: 718-430-2881; Fax: 718-430-8989; E-mail: nsibinga@aecom.yu.edu.

[2] The abbreviations used are: VSMC, vascular smooth muscle cell; Atr, atrophin; GAPDH, glyceraldehyde-3-phosphate dehydrogenase; MTOC, microtubule organizing center; siRNA, small interfering RNA; qRT, quantitative reverse transcription; EGF, epidermal growth factor; DAPI, 4′,6′-diamino-2-phenylindole.

vertebrate Fat proteins, recent reports suggest that Fat2 supports the migration of squamous carcinoma cells (16), whereas Fat4 controls the orientation of cell divisions and tubule elongation during kidney development in the mouse (17).

Genetic analysis in *Drosophila* demonstrates that Atrophin functions as a transcriptional corepressor during development, with important roles in diverse processes including segmentation and planar polarity (18). A link between Fat cadherins and Atrophin was first identified in a yeast two-hybrid screen in *Drosophila* using a fragment of the Fat cytoplasmic domain (5). Comparison of *ft* and *atrophin* mutants in *Drosophila* showed similar defects in planar polarity, and double mutants showed strongly enhanced effects on viability, indicating genetic interaction (5). Whether or not *fat-like* (*ftl*) and *atrophin* interact has not been reported.

Whereas the *Drosophila* genome encodes a single Atrophin, vertebrate genomes harbor two loci that give rise to Atr1 and two forms of Atr2: a long form (Atr2L, also known as RERE) and a short form (Atr2S); *Drosophila* Atrophin is most like Atr2L in terms of overall structure, suggesting that this long form of the protein may reflect the ancestral gene (19). Interestingly, the Atr isoforms with extended N-terminal domains (*Drosophila* Atrophin and vertebrate Atr2L) can interact with histone deacetylases (20–22), indicating at least one mechanism by which these proteins can act as transcriptional repressors. The importance of the N-terminal sequences is supported *in vivo* by the observation that, although Atr1-null mice are viable and fertile (19), Atr2L mutant mice die around embryonic day 9.5 with defects in heart looping, telencephalon, and somite development, as well as loss of Sonic hedgehog (Shh) and fibroblast growth factor (Fgf) 8 expression from anterior signaling centers (20).

In view of our previous findings that Fat1 regulates VSMC growth and migration, we asked whether mammalian Atrs and their distinct isoforms might contribute to these Fat1-mediated effects. Our studies show that Atrs, like Fat1, are induced after arterial injury, that Atrs and Fat1 interact physically, and that, again like Fat1, they regulate migration and orientation. Interestingly, however, the different Atr isoforms have distinct effects on these cellular activities; the short Atrs, Atr1 and Atr2S, promote migration and orientation, whereas the long Atr isoform, Atr2L, inhibits these activities. Taken together, these results suggest a new framework, potentially extending from the cell surface to the nucleus, for regulation of VSMC chemotaxis in the post-injury setting.

EXPERIMENTAL PROCEDURES

Rat Carotid Artery Balloon Injury—The rat carotid artery balloon injury model was implemented as described previously (1). All of the procedures were approved by and in accordance with guidelines established by the Albert Einstein Institute for Animal Studies.

Quantitative Reverse Transcription (qRT)-PCR—Total RNA was extracted from vascular tissues or cells by homogenization in TRIzol (Invitrogen), treated with DNase I (1 units/μl; Promega), and used for first-strand cDNA synthesis. The mRNA levels were quantified in triplicate by qRT-PCR in the Mx3000P real time PCR system with the Brilliant SYBR Green qPCR kit (Stratagene). The rat and mouse *atr1*-specific primers were 5′-ATCCACTCTCACCTACACCTGCAC-3′ (forward), 5′-ATCCGGGTAAGGTGAGACCCTGAG-3′ (reverse) and 5′-ACATGCTCATCACCCATTGCACAG-3′ (forward), 5′-GCTTGTCACTCTCCTTCTTCAGGT-3′ (reverse), respectively. The mouse *atr2*-specific primers were 5′-GCCCTTCATGTTCAAGCCTGTCAA-3′ (forward), 5′-TCTTCATTGATGGGTGAGGCACGA-3′ (reverse). The rat and mouse *atr2S*-specific primers were 5′-TCCTTACCTGTAGCTGCGAGTCTT-3′ (forward), 5′-AGAAGTTCTTGCCGTACTGTCGGA-3′ (reverse) and 5′-AATTAAGACTCGCACAGCGTCCAC-3′ (forward), 5′-CTGTTCGCTGTCCTCACTGTCAAA-3′ (reverse), respectively. The rat and mouse *atr2L*-specific primers were 5′-AGATCTCCAGCTCCTGCTTTGTGT-3′ (forward), 5′-TGACGTTCATGAGTAGATGGTCCC-3′ (reverse) and 5′-CCAGTCATCAAGAATCGGGAACTC-3′ (forward), 5′-GGGCTTTAAACTCTCGAGCAGCAA (reverse), respectively. PCR cycling conditions included 10 min at 95 °C for 1 cycle followed by 40 cycles at 95 °C for 20 s, 58–62 °C for 30 s, and 72 °C for 20 s. A dissociation curve obtained for each PCR product after each run confirmed that signals corresponded to unique amplicons. The expression levels were normalized by glyceraldehyde-3-phosphate dehydrogenase (GAPDH) mRNA levels for each sample in parallel assays and analyzed using the comparative $\Delta\Delta C_t$ method (23).

Cell Culture and Transfection—Primary culture VSMCs were prepared from rat or mouse aortae and maintained as described previously (1). Human aortic VSMCs were obtained from Clonetics and cultured in Dulbecco's modified Eagle's medium supplemented with 20% fetal bovine serum. VSMC phenotype was validated by immunocytochemistry using an antibody specific for α smooth muscle actin (1:400, Clone 1A4; NeoMarkers), and cells were used between four and eight passages from harvest. 293T and Chinese hamster ovary cell lines (American Tissue Type Collection) were cultured in the medium according to the supplier's recommendations. Angiotensin II, dexamethasone, and transforming growth factor-β were obtained from Sigma, and basic fibroblast growth factor, platelet-derived growth factor BB, interferon-γ, and interleukin-1β were from U.S. Biological. In stimulation experiments, the cells were rendered quiescent by incubation in medium containing 0.4% horse serum for 72 h prior to the addition of fetal bovine serum or other stimulus. Control cultures received an equivalent amount of vehicle. Total cellular protein or total RNA was extracted at designated time points. In transfection experiments, FuGENE 6 (Roche Applied Science) or TransIT-LT1 reagent (Mirus) were used according to the manufacturers' protocols.

Northern Analysis—Total RNA (10 μg) was fractionated on 1.2% formaldehyde-agarose gels and transferred to nitrocellulose filters. A rat Atr2 cDNA probe, corresponding to nucleotides 4495–4922 in GenBank^{TM} entry NM_053885, was generated by PCR, random primed in the presence of ^{32}P-labeled dCTP, and hybridized to the filters in QuikHyb (Stratagene). The filters were washed to high stringency at 55 °C in buffer containing 30 mmol/liter sodium chloride, 3 mmol/liter sodium citrate, and 0.1% SDS. Autoradiography was performed with Kodak XAR film at −80 °C for 48 h.

5′-Rapid Amplification of cDNA Ends—To define the 5′ end of the mouse *atr2S* transcript, we performed 5′-rapid amplification of cDNA ends using Ambion mouse embryo rapid amplification of cDNA ends-ready cDNA according to the manufacturer's instructions. The *atr2* gene-specific primers were: 5′-TGGGAGACGTGCTGCGATTA-3′ (outer primer) and 5′-ATGCAGCCTCTTCCTTCACCTT-3′ (inner primer). Amplified cDNA products were cloned and sequenced by standard methodology. This sequence will be supplied as supplemental data.

Western Analysis—The cells were homogenized, and the proteins were extracted in radioimmunoassay buffer containing protease inhibitors and resolved by SDS-PAGE with 3–8% Tris acetate or 8% Tris-glycine gels (Invitrogen). The proteins were transferred electrophoretically onto ImmobilonP membranes (Millipore), which were incubated with antisera or monoclonal antibodies specific for Fat1 (1), Atr1 (1:100, A-19; Santa Cruz), FLAG M2 (1:5000; Sigma), or c-Myc (1:100, 9E10; Santa Cruz). Equivalent protein loading was evaluated with anti-Actin (1:100, C-11; Santa Cruz) antibody.

cDNA Constructs—The DelN-Fat1 construct (13) encodes an N-terminal truncated form of human Fat1 (amino acid residues 3987–4590) in which all the cadherin domains, one EGF motif, and the laminin A-G domain have been removed, and part of the extracellular and all of the transmembrane and intracellular domains (IC) are retained. We generated a similar construct by RT-PCR. A 3XFLAG sequence was integrated in frame into the N-terminal of the cDNA, and the resulting product was subcloned into the p3XFLAG-CMV-13 expression vector (Sigma), yielding an N-terminally FLAG-tagged product defined at the C terminus by the native Fat1 stop codon. Derivative C-terminal truncation constructs, designated DelN-Fat1 4500, DelN-Fat1 4400, and DelN-Fat1 4300, were generated by introducing an additional stop codon at the corresponding amino acid residue (residue 4500, 4400, or 4300) by QuikChange site-directed mutagenesis (Stratagene). The full-length cDNAs encoding human Atr1 and Atr2L (long form, amino acids 1–1506) were obtained from Open Biosystems and subcloned into pCMV·SPORT6 (Invitrogen) and pcDNA-DEST40 (Invitrogen), respectively. These cDNA inserts were also cloned in frame into the pCS2–6XMyc vector to provide C-terminal Myc epitope tags and into the pEGFP-C2 vector (Clontech) to provide N-terminal EGFP epitope tags. The Atr2S (short form, amino acids 495–1506) cDNA was obtained by RT-PCR and subcloned similarly into the pCS2–6XMyc and pEGFP-C2 vector. All of the constructs were confirmed by sequencing.

RNA Interference—The mouse Fat1 siRNA has been described previously (1). The mouse *atr* siRNAs (Sigma/Proligo) were designed to target 21-nucleotide sequences derived from *atr1* (GenBank™ accession number NM007881, starting at positions 719 (GAATGCTAGTGGAGGTGTT), 905 (GAGCTTACCTTCTGCACCA), and 1297 (CTAGTATGTCTGTCTCTAA)), *atr2* (GenBank™ accession number XM204015, starting at positions 689 (CTGATTATGTTGACACCTA); 1116 (CAGTTATGATGCCGGCAAA), and 4622 (CAAGTCAGGAGGATTATTA)). Control siRNA included scrambled derivatives of the *atr1* 1297 sequence, *atr2* 4622 sequence, an unrelated siRNA based on the *Renilla* luciferase sequence, and a negative control siRNA (Qiagen). siRNA was transfected with X-tremeGENE reagent (Roche Applied Science) according to the manufacturer's recommendations. Knockdown efficiency was assessed by Western analysis or qRT-PCR.

Coimmunoprecipitation—Specific proteins were immunoprecipitated by incubating 300–500 μg of precleared whole cell lysates in immunoprecipitation buffer with 2–5 μg of the corresponding antibodies or normal IgG control at 4 °C for 2 h, followed by incubation with protein G agarose (Invitrogen) at 4 °C overnight with gentle agitation. After extensive washing, the immune complexes were recovered by boiling in sample buffer, and the proteins were detected by Western analysis.

Immunocytochemistry—The cells were plated on chamber slides (Becton-Dickinson), fixed, stained, and photographed by epifluorescent microscopy as previously described (1). Primary antibodies were used at the dilutions indicated: anti-Fat1, 1:1000; anti-Atr1 (A-19; Santa Cruz), 1:100; anti-RERE (REREF1H8; Abcam) 1:50; and anti-Myc (9E10; Santa Cruz), 1:100. After incubating with AlexaFluor-conjugated secondary antibody (1:2000; Molecular Probes) and counterstaining with DAPI, the samples were mounted (Supermount medium; Biogenex) on glass slides, and the signals were visualized using an inverted fluorescent microscope (model IX70; Olympus) equipped with 20×/NA 0.4 and 40×/NA 0.6 LWD objectives and standard fluorescent filter sets, a CCD camera (SensiCam; Cooke), and IPLab software (Scanalytics). Subsequent image processing was performed using Photoshop CS3 and Illustrator CS3 (Adobe Systems). Routine control experiments included omission of the primary antibodies.

Lentivirus Preparation and Transduction—Lentivirus was produced using the Virapower Lentiviral kit (Invitrogen) according to the manufacturer's directions. Briefly, cDNA encoding full-length of human Atr1 was cloned into the pLenti6-V5-DEST vector, and virus was generated in the 293FT viral packaging cell line. Equal titers of test or vector control virus were used in subsequent experiments. Mouse VSMCs were infected with virus-containing supernatant in the presence of polybrene, and stably transduced cells were selected with Blasticidin. A total of 16 clones were isolated, and Atr1 expression levels were detected by Western blot.

Cell Proliferation Assay—To evaluate DNA synthesis, 1×10^4 cells plated on four-chamber type I collagen-coated chamber slides (Becton Dickinson) were transfected with siRNA, serum-starved (0.4% horse serum) for 48 h, and then stimulated with 10% fetal bovine serum. Bromodeoxyuridine (10 μM, Sigma-Aldrich) was added to cells for 6 h before harvest after 24 h of stimulation. The cells were washed in phosphate-buffered saline, fixed in 4% paraformaldehyde, treated with HCl, and stained sequentially with anti-bromodeoxyuridine antibody (1:200; Abcam) and AlexaFluor 555-conjugated secondary antibody (1:2000; Molecular Probes). The cells were counterstained with DAPI (Molecular Probes).

Cell Migration Assay—Cell migration was assessed by 1) *in vitro* scratch wounding of monolayers and 2) with Transwell 24-well cell culture inserts with 8-μm pores (Costar), as described previously (1). For the former, cellular progress was photographed and quantitated by planimetry of the denuded

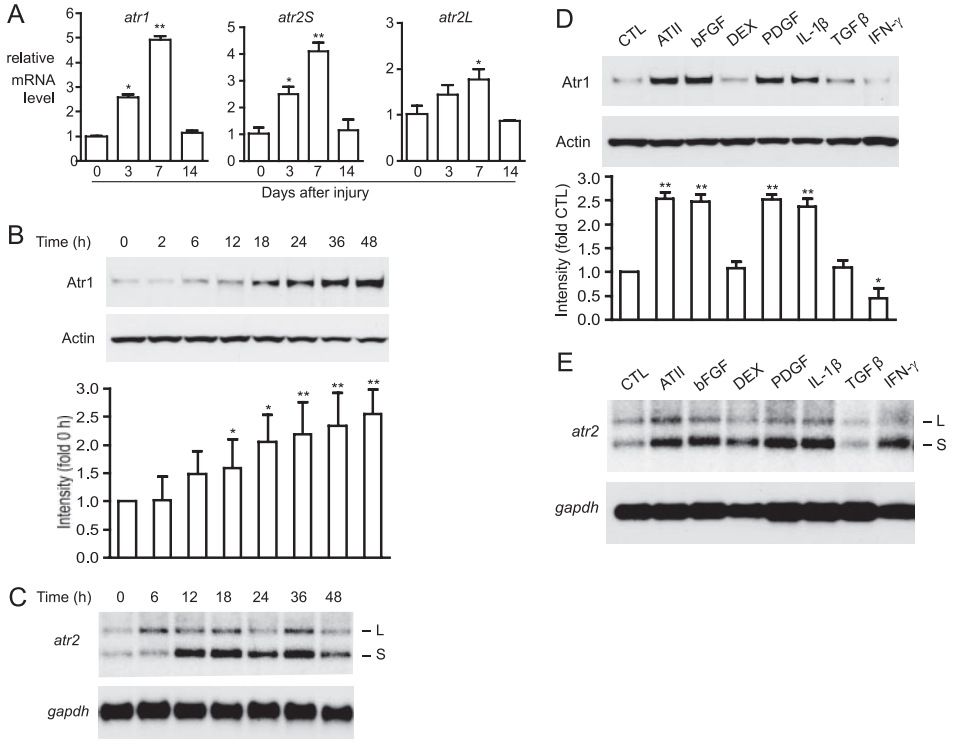

FIGURE 1. **Atr expression in normal and balloon-injured rat carotid arteries and VSMCs.** *A*, qRT-PCR analysis of *atr1*, *atr2S*, and *atr2L* mRNA levels. Test mRNA levels were corrected relative to *gapdh* mRNA, with day 0 (no injury) set = 1. *, $p < 0.05$; **, $p < 0.01$ *versus* day 0. The data show the means ± S.E. *B* and *C*, rat VSMCs were serum-deprived for 72 h, stimulated by 10% fetal bovine serum, harvested for protein or total RNA extraction after indicated time points, and probed for Atr1 expression by Western analysis (*B*) or probed for *atr2S* and *atr2L* expression by Northern analysis (*C*). The blots were also reprobed for Actin or *gapdh* as loading reference. *D* and *E*, rat VSMCs were serum-deprived for 72 h, stimulated by specific factors, harvested for protein or total RNA extraction after 24 h, and probed for Atr1 expression by Western analysis (*D*) or probed for *atr2S* and *atr2L* expression by Northern analysis (*E*). The blots were also reprobed for Actin or *gapdh* as loading reference. Specific factors and concentrations were vehicle control (*CTL*); angiotensin II (*ATII*), 10^{-6} mol/liter; basic fibroblast growth factor (*bFGF*), 20 ng/ml; dexamethasone (*DEX*), 1 μmol/liter; platelet-derived growth factor BB (*PDGF-BB*), 20 ng/ml; interleukin-1β (*IL-1β*), 10 ng/ml; transforming growth factor-β (*TGF-β*), 10 ng/ml; or interferon-γ (*IFN-γ*), 300 units/ml. The data are representative of three independent experiments. For Western analysis, one representative result is shown on the *top panel*, and densitometric quantitative analysis is shown on the *bottom panel*, with *error bars* indicating the S.E. *, $p < 0.05$; **, $p < 0.01$ *versus* 0 h or CTL.

area and converted to distance migrated using Image J software. For Transwell assays, quiescent cells were harvested and added (1×10^5/well) to the insert. Culture medium containing 10% fetal bovine serum as chemotactic agent was added to the lower chamber. After 10 h, nonmigrating cells were removed from upper filter surfaces, and the filter was washed, fixed, and stained. We then photographed fifteen randomly selected 100× fields and counted cells that had migrated to the underside of the filter.

Microtubule Organizing Center (MTOC) Orientation Assay—The cells were grown to confluence, and the monolayer was denuded in a linear stripe using a pipette tip. The cells were fixed 16 h later with 4% paraformaldehyde, and the MTOC was localized by immunolabeling using anti-pericentrin antibody (1:1000, Abcam) and a secondary goat anti-rabbit labeled with Alexa 488 dye (Invitrogen). Cell nuclei and cytoskeleton were identified with DAPI and rhodamine-phalloidin stains, respectively (Invitrogen). The signals were visualized by epifluorescent microscopy, and cells in which the MTOC localized within the 120° sector facing a line parallel to the wound margin were scored positive. At least 100 cells were examined for each condition.

Statistical Analysis—Experiments were repeated a minimum of three times. Comparisons between two groups were analyzed by Student's *t* test ($p < 0.05$), and comparisons between three or more groups were assessed by analysis of variance with a Bonferroni/Dunn post hoc test ($p < 0.05$). The data are presented as the means ± S.E.

RESULTS

Atr1 and Atr2 Are Induced after Vascular Injury and by Growth Factors—Like *fat1* (1), both *atr1* and *atr2* transcripts increased after rat carotid artery balloon injury. For each isoform, mRNA levels peaked 7 days after injury, with levels ~5-, 4-, and 1.8-fold over base line for *atr1*, *atr2S*, and *atr2L*, respectively (Fig. 1*A*). We also found induction of Atr1 protein in response to serum (Fig. 1*B*), again reminiscent of the pattern we found with Fat1 (1). Although a similar analysis of Atr2 protein was limited by lack of effective antibodies, Northern analysis showed two distinct *atr2* transcripts, which we designate *atr2L* and *atr2S*, consistent with previous observations (19). Both *atr2L* and *atr2S* transcripts increased in response to serum stimulation, albeit with somewhat different kinetics and a greater induction of *atr2S* (Fig. 1*C*). Interestingly, relative *atr2* isoform levels showed some cell type dependence, because we found a preponderance of the *atr2S* isoform in VSMCs and of the *atr2L* isoform in Chinese hamster ovary cells (supplemental Fig. S1). We also tested the response of Atrs to individual factors with known regulatory roles in vascular remodeling. Atr1 protein levels increased ~2.5-fold in VSMCs treated with angiotensin II, basic fibroblast growth factor, platelet-derived growth factor BB, and interleukin-1β and decreased in cells treated with interferon-γ (Fig. 1*D*). These treatments, like serum treatment, induced *atr2S* more strongly than *atr2L*. Among these factors, the effect of interferon-γ was unique, in that it decreased Atr1 expression while preferentially inducing *atr2S* mRNA (Fig. 1*E*).

Atr Proteins Colocalize with Fat1 in Different Subcellular Locations—We then determined the subcellular localization of these proteins. Atr1 staining was prominent in the perinuclear area, with less intense signal present at cell leading edges and within the nucleus. Overall, the pattern of Fat1 staining was quite similar, although the Fat1 signal was more prominent at the leading edges (Fig. 2*A*). Overlap of these signals was apparent in the perinuclear area and at cell-cell junctions and leading edges (Fig. 2*A*, *Merge*). Atr2 staining was apparent in cell nuclei

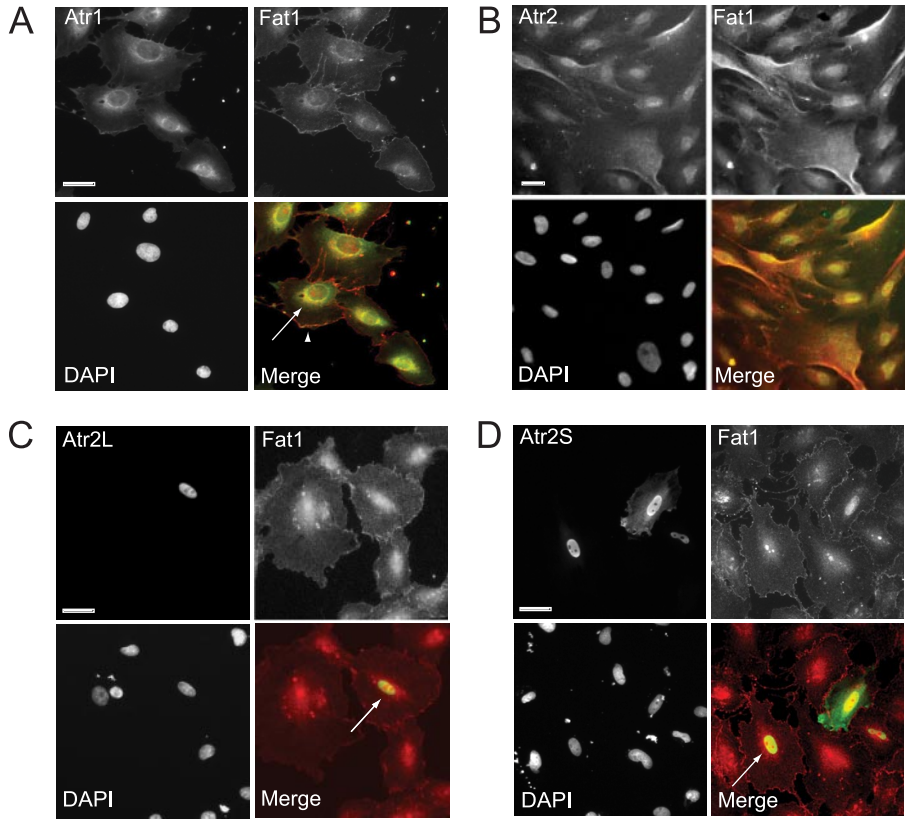

FIGURE 2. **Colocalization of Atrs and Fat1 in VSMCs.** Shown is immunofluorescence analysis of Fat1 and endogenous rat Atr1 (*A*), endogenous human Atr2 (*B*), transfected, epitope-tagged rat Atr2L (*C*), and transfected, epitope-tagged rat Atr2S (*D*). In the merged color images, Fat1 staining is *red*, Atr staining is *green*, and areas of colocalization (*arrows* and *arrowhead*) are *yellow*. Nuclei stained with DAPI are also shown. Fat1, Atr1, and Atr2 were detected with specific antibodies against the respective proteins; epitope-tagged Atr2 isoforms were detected with anti-c-Myc antibody. *Scale bars*, 10 μm.

and diffusely throughout the cytoplasm and showed overlap with Fat1 in these areas (Fig. 2*B*). To assess the distribution of the 2 Atr2 isoforms, we transfected cells with constructs encoding epitope-tagged Atr2L or Atr2S. The former localized exclusively to the nucleus, where some overlap with Fat1 was evident (Fig. 2*C*, *Merge*). The epitope-tagged Atr2S isoform, on the other hand, was present in the cytoplasm and at cell borders and coincided with Fat1 signal within the nucleus and at cell-cell borders (Fig. 2*D*). Although transfection, epitope tagging, and overexpression can all spuriously affect protein localization, our findings with liposome-mediated transfection of these C-terminal tagged constructs were consistent with studies of endogenous protein (Fig. 2*B*) as well with studies using N-terminal tags (supplemental Fig. S2) and electroporation (not shown).

Atr Proteins Coimmunoprecipitate with Fat1—To evaluate possible physical association of Fat1 and Atrs, we immunoprecipitated endogenous Atr1 from VSMC lysates and probed for Fat1, which was readily detectable in these immunoprecipitates, but not in control samples (Fig. 3*A*). This finding using whole cell lysates is consistent with a direct Atr-Fat1 interaction or indirect association based on coexistence in larger multi-protein complexes. We then mapped the domains required for this association. Progressive deletions starting from the Fat1 C terminus (Fig. 3*B*) were tested by cotransfection with Myc epitope-tagged Atr1 or Atr2L and FLAG-tagged Fat1 derivatives. As shown in Fig. 3*C*, Fat1 constructs with full-length and slightly truncated cytoplasmic domains retained the ability to coimmunoprecipitate with Atrs (*lanes 4* and *5*), whereas those with deletions between amino acids 4500 and 4400 lost much of this activity; further deletions to amino acid 4300 eliminated coimmunoprecipitation. We obtained similar results in studies with the interleukin 2R-mouse $Fat1_{IC}$ domain fusion protein series of internal deletion constructs (1); these experiments implicated both the FC1 (amino acids 4297–4395) and FC2 (amino acids 4395–4497) domains (supplemental Fig. S3). These results point to Fat1 sequences overlapping domains FC1 and FC2, which we previously also identified as interacting domains for β-catenin (1). Residues critical for some interactions with Atrs have been localized to the Atr-box (Fig. 3*D*) in the C-terminal domain of Atr (21). We found that these residues were also important for the interaction of Atr1 and Atr2 with Fat1, because mutation of two conserved leucines within the Atr-box caused a substantial reduction in the binding (Fig. 3*E*, *lane 3 versus lane 4* and *lane 5 versus lane 6*).

Selective Inhibition of Atr Expression by siRNA—We then developed effective siRNA reagents to allow direct testing of the effects of loss of Atr function in VSMCs. *Atr1*-selective siRNAs to three distinct targets were transfected into cells at high efficiency and evaluated by Western analysis and qRT-PCR. In each individual case, Atr1 expression was substantially reduced, but a pool of the siRNAs had no additional effect (Fig. 4*A*). Knockdown mediated by siRNA 1297 was highly efficient at 2 and 3 days after transfection, with some loss of effect by 6 days (Fig. 4*B*). For siRNAs targeting *atr2*, we detected knockdown by qRT-PCR caused by a lack of an effective antibody for Atr2 Western analysis. siRNAs targeting the 5′ region of *atr2* (amino acids 689 and 1116) selectively decreased *atr2L* transcripts, whereas 3′ region (amino acid 4622) or pooled siRNAs knocked down both *atr2L* and *atr2S* transcripts (Fig. 4*C*). Again, knockdown of ~80% by a single siRNA, 4622, persisted through 2 and 3 days after transfection, with some loss of effectiveness by 6 days (Fig. 4*D*). These siRNAs did not show unintended targeting of other *atr* isoforms (supplemental Fig. S4).

Atr Knockdown Does Not Affect VSMC Growth—Fat1 knockdown allows robust increases in VSMC proliferation (1). In view of the Fat1 and Atr interactions characterized in Figs. 2 and 3, we speculated that the loss of Atr might also affect VSMC growth. We used siRNA-mediated knockdown of Atr1 and Atr2, separately and together, and evaluated proliferation by

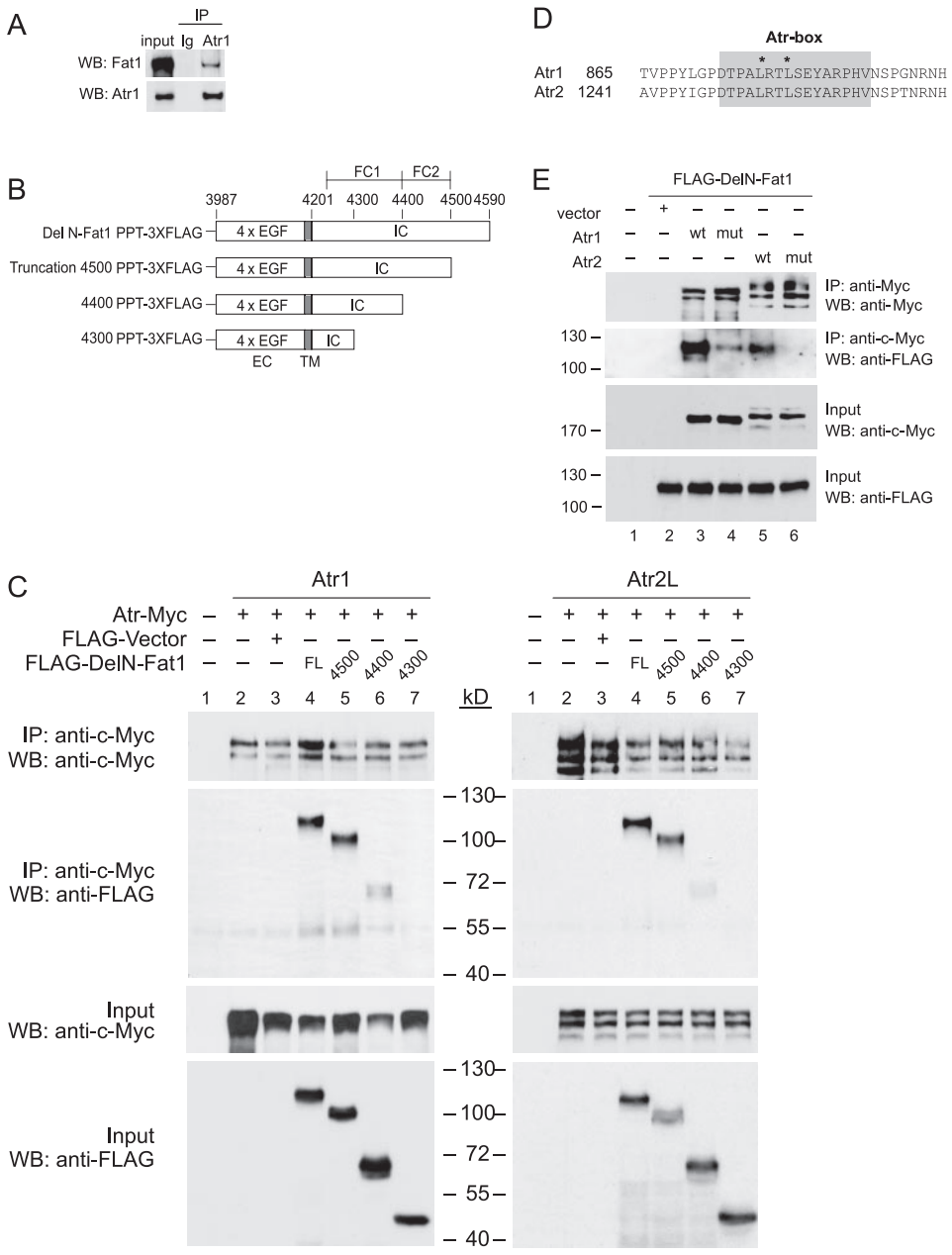

FIGURE 3. **Fat1 and Atr interact physically.** *A*, coimmunoprecipitation (*IP*) of endogenous Fat1 and Atr1. Rat VSMC lysates were incubated with anti-Atr1 specific or nonimmune goat IgG (*Ig*), and the immunoprecipitated complexes were analyzed by Western analysis (*WB*) for Fat1 and Atr1, as indicated. *B*, schematic of the DelN-hFat1 series of C-terminal deletion constructs used for coimmunoprecipitation mapping studies. Numbering refers to full-length human Fat1 amino acid sequence. *EGF*, EGF-like repeats; *EC*, extracellular; *TM*, transmembrane; *IC*, intracellular. *FC1* and *FC2* refer to conserved cadherin interaction domains (see Ref. 1). *C*, coimmunoprecipitation and Western analysis of transfected FLAG epitope-tagged DelN-hFat1 and Myc-epitope tagged Atr proteins in 293T cells, showing interaction of Fat1 constructs with Atr1 (*left*) and Atr2L (*right*). The cell lysates were tested to confirm efficient expression of all transfected constructs (input, *bottom panels*). *D*, schematic showing highly conserved Atr-box sequence in Atr1 and Atr2, and location of mutated residues. *E*, coimmunoprecipitation and Western analysis of transfected FLAG epitope-tagged DelN-hFat1 and Myc-epitope tagged Atr proteins, with wild type (*wt*) or mutated Atr-box sequences. The cell lysates were tested to confirm efficient expression of all transfected constructs (input, *bottom panels*). The data are representative of three independent experiments.

bromodeoxyuridine incorporation. These studies provided, however, no evidence that changes in Atr1 or Atr2 expression affected proliferation (supplemental Fig. S5).

Loss of Atr1 Impairs, and Loss of Atr2L Enhances, VSMC Migration—Decreased Fat1 expression has also been linked to impaired cell migration (1, 13, 14, 24). We used siRNA knockdown to test how Atr expression affected the ability of VSMC to migrate in response to denudation injury of a confluent cellular monolayer. Knockdown of Atr1 (*atr1* siRNA 1297) decreased the distance that VSMC migrated after injury; an additive effect was seen when expression of both Fat1 and Atr1 was inhibited (Fig. 5*A*). We also examined the physical distribution of Atr1 and Fat1 within VSMCs responding to monolayer injury. The large *arrow* in Fig. 5*B*, drawn orthogonally to the line of denudation, represents the presumed direction of migration. Atr1 and Fat1 were both apparent at filopodial and lamellipodial tips extending toward the denuded area, and Atr1 colocalized with F-actin-rich structures (arrowheads).

To extend this analysis, we tested Atr2 effects on migration. Interestingly, *atr2* siRNA 4622, which targets a site common to both short and long *atr2* isoforms, had no effect on migration, but *atr2* siRNAs 689 and 1116, which target sites present only in *atr2L* transcripts, each increased the distance that cells migrated (Fig. 5*C*, *left panel*). Further evaluation showed that *fat1*-specific siRNA cotransfected with *atr2* siRNA 4622 inhibited migration and prevented the increased migration seen with the *atr2* siRNA 689 (Fig. 5*C*, *center panel*). Knockdown targeting all Atrs yielded no net change in migration (Fig. 5*C*, *right panel*).

Studies using Transwell assays of cell migration yielded results (Fig. 5*D*) that were qualitatively similar to those obtained with monolayer denudation. In addition, we studied the effect of combined knockdown of Atr1 and Fat1, which caused a modestly more significant decrease in cell migration compared with individual knockdown (Fig. 5*D*, *upper left panel*). Together, these findings suggest that Atr1, like Fat1, promotes VSMC migration, whereas Atr2L inhibits it, with the latter effect requiring Fat1 expression. Because knockdown of both Atr2 isoforms did not change migration, we suggest that Atr2S, like Atr1, promotes migration, but this effect is masked by concurrent loss of Atr2L with siRNAs targeting sites shared by both isoforms. To

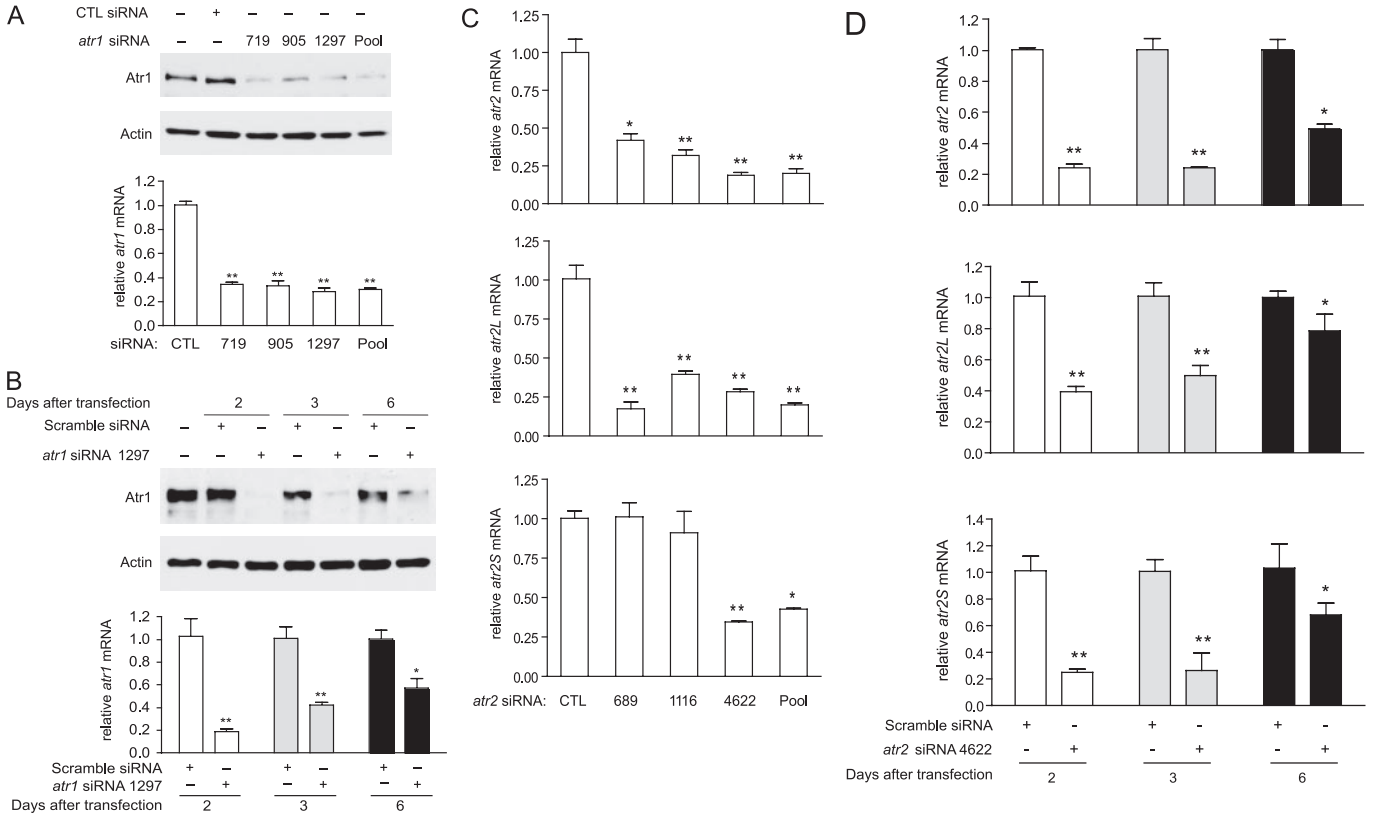

FIGURE 4. **siRNA-mediated knockdown of Atr1 and Atr2 in mouse VSMCs.** Atr expression in cells transfected with control (*CTL*) or *atr*-specific siRNAs is shown; + denotes equivalent siRNA to achieve final concentration of 0.2 μmol/liter. *A*, Western (*top panels*) and qRT-PCR (*bottom panel*) analysis of Atr1 expression 48 h after transfection of individual or pooled siRNAs. *B*, efficacy of *atr1*-specific siRNA 1297 from 2–6 days after transfection estimated by Western (*top panels*) and qRT-PCR (*bottom panel*) analysis. *C* and *D*, qRT-PCR analysis of *atr2*, *atr2L*, and *atr2S* mRNA expression 48 h after transfection of individual or pooled siRNAs (*C*) or from 2–6 days after transfection with *atr2*-specific siRNA 4622 (*D*). Western blots were reprobed for Actin expression as reference. mRNA levels were corrected relative to *gapdh* mRNA levels, with control siRNA set = 1. *, $p < 0.05$; **, $p < 0.01$ *versus* CTL. The data show the means ± S.E.

our knowledge, Atr proteins have been not been previously linked to regulation of migration.

Loss of Atr1 Impairs, and Loss of Atr2L Enhances, VSMC Orientation—Work in *Drosophila* supports a role for Atr in the establishment of planar cell polarity (5). VSMCs in culture do not normally show planar polarization but do respond to injury of the cellular monolayer with directed migration into the denuded area (25, 26). We hypothesized that perturbation of VSMC orientation toward the denuded area could contribute to the changes in net migration that we found with knockdown of Atr1 or Atr2L (Fig. 5). To test this idea, we performed scratch wound injury of confluent mouse VSMC monolayers treated with *atr* siRNAs and assessed cellular orientation by staining the MTOC with a pericentrin-specific antibody (supplemental Fig. S6). Knockdown of Atr1 or Fat1 decreased the percentage of cells along the margin that oriented toward the wounded area; combined Atr1-Fat1 knockdown yielded additional misorientation (Fig. 6*A*); Targeting of *atr2S* and *atr2L* with siRNA 4622 had no net effect on orientation, but knockdown with *atr2* siRNA 689, which selectively targets *atr2L*, caused a significant increase in the percentage of VSMCs oriented toward the wound area; this increase was eliminated by concurrent knockdown of Fat1 (Fig. 6*B*). Knockdown of both Atr1 and Atr2 had no net effect on orientation (Fig. 6*C*). Overall, these findings echo the effects of *atr1*- and *atr2*-selective siRNAs on migration and support the idea that control of cellular orientation toward the denuded area contributes to the migration effects of Atr knockdown measured in our scratch wound assays.

Overexpression of Atr1 Enhances VSMC Migration and Orientation—To complement the loss-of-function studies described in Figs. 5 and 6, we tested the effect of increased Atr1 expression. For this analysis, we transduced mouse VSMCs with a lentivirus encoding full-length Atr1, selected individual colonies, and identified several clonal lines stably expressing different levels of Atr1 (Fig. 7*A*). We used line Atr1–2, with a modest level of overexpression, and line Atr1–6, with strong overexpression, in Transwell and orientation assays. Strong Atr1 overexpression yielded a significant increase in migration (Fig. 7*B*) and orientation (Fig. 7*C*) compared with VSMCs transduced with vector alone, whereas modest overexpression showed a nonsignificant trend in the same direction.

DISCUSSION

Atrs were first identified because of their pathogenetic role in dentatorubral-pallidoluysian atrophy, a clinical syndrome in which polyglutamine expansions of Atr1 lead to progressive neurodegenerative disease (27–29). Recent studies show that Atrs have essential functions in metazoan development. *Drosophila* embryos lacking maternal Atrophin display complex developmental phenotypes, with failures of segmentation, dorsoventral patterning, and neuro-

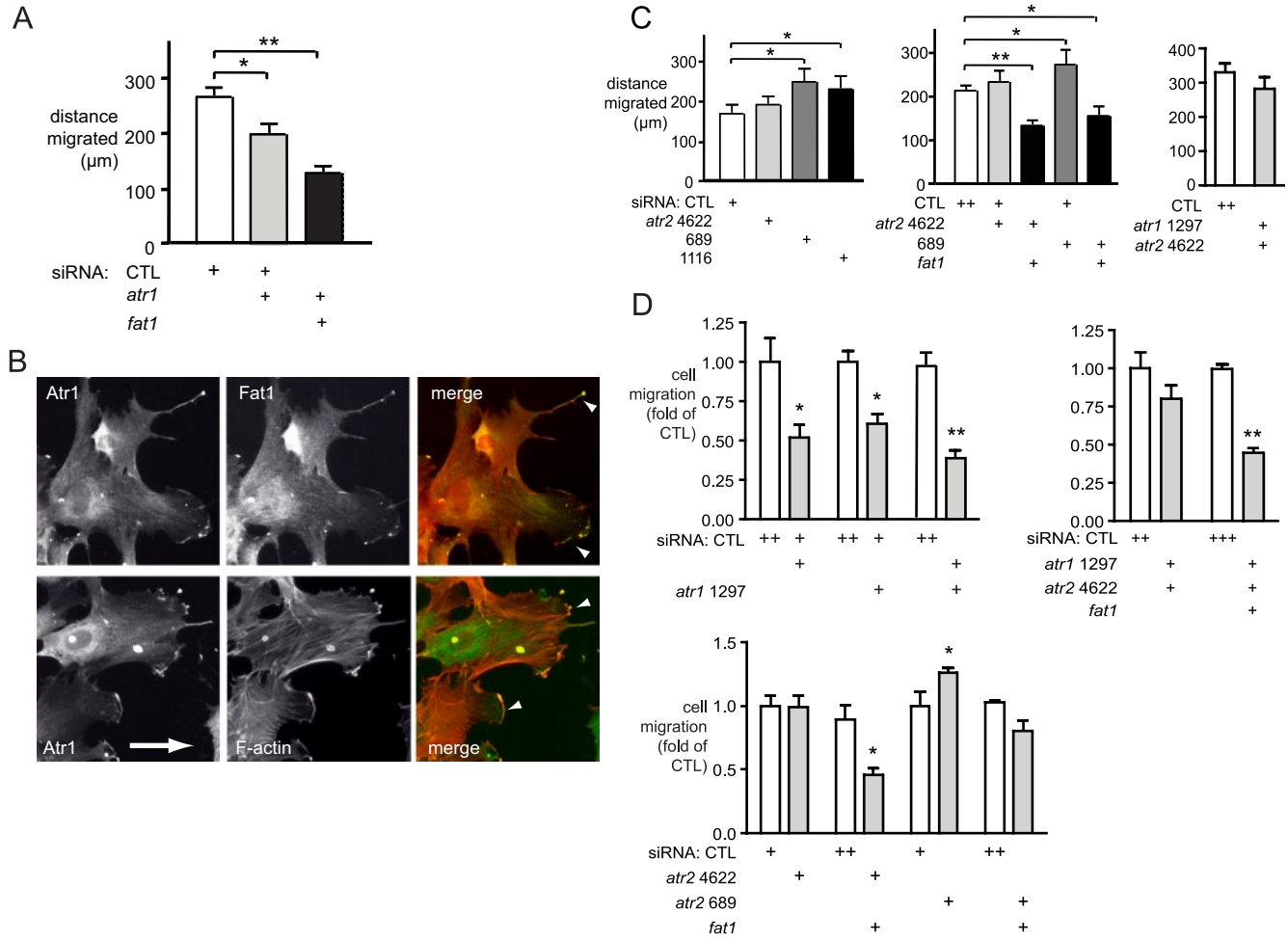

FIGURE 5. **Regulation of VSMC migration by Atrs and Fat1 knockdown.** *A*, scratch wounding migration assay of mouse VSMCs transfected with control (*CTL*) or specific *atr1* siRNA alone or in combination with *fat1* siRNAs, as indicated. After 48 h, the confluent monolayers were injured with a pipette tip. The area of the denuded monolayer covered by cells was recorded immediately and after 24 h by photomicrography of eight matched fields/sample. Distance migrated during this interval was calculated by planimetry using Image J. The data show the means ± S.E. *, $p < 0.05$; **, $p < 0.01$. *B*, localization of Atr1 in migrating VSMC. Human VSMCs migrating in a wounding assay were fixed 16 h and doubly stained with antibodies specific for Atr1and Fat1(*top panels*) or Atr1 and filamentous actin (F-actin, rhodamine-phalloidin) (*bottom panels*). In the merged color images, Atr1 staining is *green*, Fat1 or F-actin staining is *red*, and areas of colocalization (*arrowheads*) are *yellow*. The *arrow* points orthogonally to the wound edge. *C*, scratch wounding migration assay of mouse VSMCs transfected with CTL or specific *atr2* siRNA along or in combination with *fat1* or *atr1* siRNAs, as indicated. The method and analysis are as described above, except that migration proceeded for 30 h for the *right panel*. *D*, Transwell migration assay of mouse VSMCs transfected with control or specific *atr* or *fat1* siRNA along or in combination, as indicated. Fifteen photomicrographic fields were counted per condition, and the values were averaged for each filter. The data show the means ± S.E. *, $p < 0.05$; **, $p < 0.01$, *versus* control. The data are representative of three independent experiments.

genesis, and mosaic adult flies with clonal lineages bearing *atrophin* mutations show pleiotropic effects, including accumulation of ectopic wing vein material, notal clefts, nonautonomous planar polarization defects in the eye (18), and position-dependent patterning defects in the leg, in which ventral Atrophin-deficient clones exhibit lateral-distal phenotypes (18, 30). Similarly, mice lacking Atr2L show defective patterning in multiple aspects of early development, with specific failure in ventralization of the anterior neural plate, loss of heart looping, and irregular partitioning of somites (20). On the other hand, Atr1, despite its association with clinical neurodegenerative disease, is not required for developmental patterning, perhaps because of functional redundancy with the other vertebrate short form of Atr, Atr2S (19).

Although Atrs have frequently been described as transcriptional corepressors, the molecular basis for Atr function is not entirely clear. A model to explain bidirectional and isoform-dependent Atr transcriptional function has recently been proposed, in which interaction with histone deacetylases confers transcriptional repressive activity to the isoforms that bear extended N-terminal domains (*Drosophila* Atrophin and vertebrate Atr2L), whereas C-terminal association with the histone acetyltransferase p300 (all Atr isoforms) supports positive transcriptional activity, as seen with Atr1 and Atr2S (19). Nevertheless, a number of examples that do not fit this relatively straightforward model have been reported: 1) Atr1 (a short form) tethered to DNA recruits repressive activity in cultured cells (18, 31, 32); 2) Atr1 and *Drosophila* Atrophin (a long form) each repress transcription when tethered to DNA *in vivo* (18); and 3) *Drosophila* Atrophin has been characterized as positive regulator of gene expression in the proximoventral leg (30). Several possible explanations for these discrepancies can be suggested. Atrs may associate with additional unknown tran-

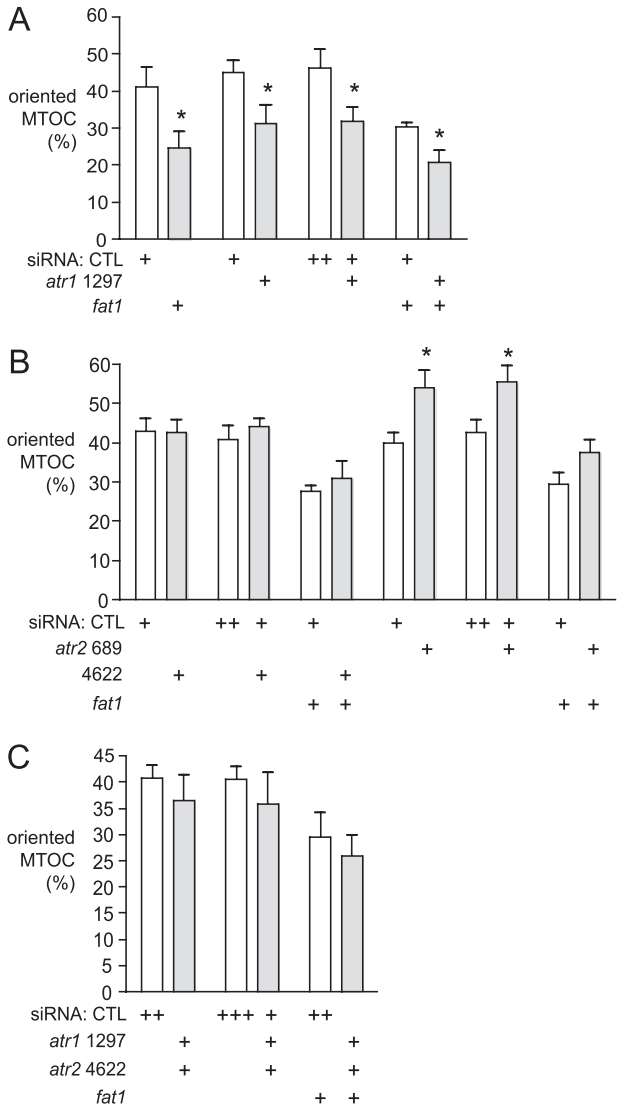

FIGURE 6. **Effect of Atr and Fat1 knockdown on VSMC orientation in scratch-wounded monolayers.** Mouse VSMCs were fixed 16 h after wounding and stained with an anti-pericentrin antibody to show MTOCs. Cellular orientation along the injured margin was scored positive if the MTOC was located within the 120° sector facing toward the denuded area (see supplemental Fig. S6). The graphs show the percentage of cells along the wound margin showing positive MTOC orientation, and the effects of inhibition of Fat1 or Atr1 alone or knockdown of both (*A*), inhibition of both Atr2S and Atr2L (siRNA 4622) or Atr2L alone (siRNA 689), or in combination with knockdown of Fat1 (*B*), and inhibition of Atr1 in combination with knockdown of both Atr2S and Atr2L (siRNA 4622), or plus knockdown of Fat1 (*C*). At least 200 cells were scored per condition. The values represent the means ± S.E. *, $p < 0.05$, *versus* control (*CTL*). The data are representative of three independent experiments.

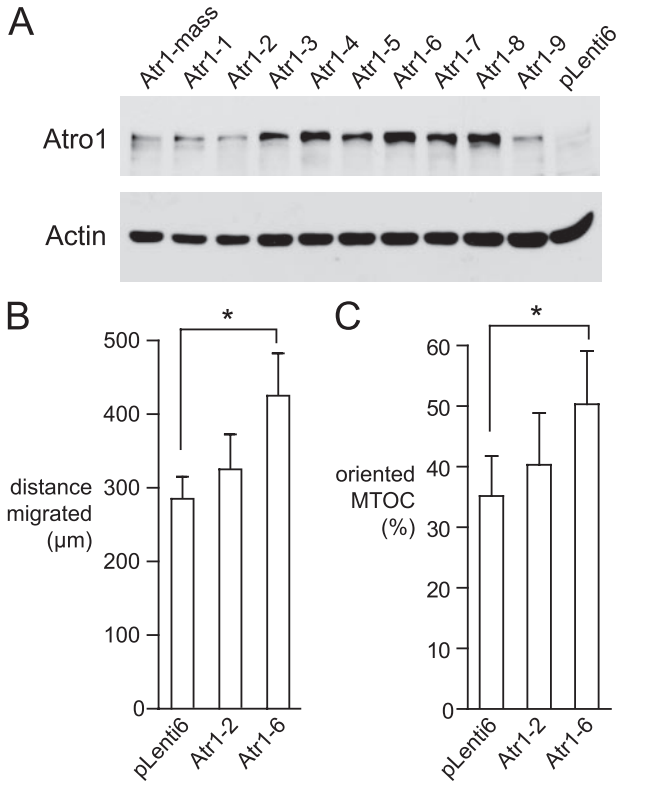

FIGURE 7. **Effect of Atr1 overexpression on VSMC migration and orientation in scratch-wounded monolayers.** *A*, Western analyses of Atr1 overexpression in mouse VSMC stable transfectants. After Blasticidin selection, cell lysates from a vector-transfected clone (*pLenti6*), Atr1 mass cultures (*Atr1-mass*) as well as several Atr1 clonal cell lines (*Atr1–1* to *Atr1–9*, respectively) were immunoblotted with antibody against Atr1. The blot was also probed for Actin as loading reference. *B*, effect of Atr1 overexpression on VSMC migration in scratch-wounded monolayers. Atr1–2, Atr1–6, and pLenti6 vector alone mouse VSMC were allowed to migrate 28 h after wounding of monolayer, and the migration distance was evaluated as described above. The data show the means ± S.E. *, $p < 0.05$. *C*, effect of Atr1 overexpression on VSMC orientation in scratch-wounded monolayers. Atr1–2, Atr1–6, and pLenti6 vector alone mouse VSMC were fixed 16 h after wounding and stained to show MTOCs. The data show the means ± S.E. *, $p < 0.05$. The data are representative of three independent experiments.

scriptional regulators, interactions may be controlled by post-translational mechanisms not yet identified, or some of the reported effects may be indirect. In addition, short Atr isoforms are found outside the nucleus (Fig. 2), but whether they have specific functions in the cytoplasm is unknown.

The link between Atrophin-mediated gene regulation and the cellular effects that underlie critical Atrophin roles in development and neurodegenerative disease are also not fully understood. Lost expression of a diffusible signal may underlie planar polarity defects seen in the *Drosophila* eye with loss of Atrophin function (5). In Atr2L-deficient mice, misregulation of Shh and Fgf8 expression during development may undermine proper formation and function of critical anterior midline, anterior neural ridge, and apical ectodermal ridge signaling centers (20). Increased Atr levels appear to be particularly toxic in neural tissues, because increased apoptosis was found in neuroblastoma cells with increased Atr2L expression (33) and in *Drosophila* neurons with increased Atrophin expression that results from the loss of negative regulation by the micro RNA mIR-8 (34).

In the present study, we found that Atrs are induced in injured arteries and in cultured VSMCs exposed to growth factors. In view of previous similar findings with the atypical cadherin Fat1 (1) and the reported interaction of *Drosophila* Atrophin and Fat (5), we sought to test the role of Atrs in the prominent VSMC activities provoked by these *in vivo* and *in vitro* manipulations. Although Fat1 inhibits growth and enhances migration of VSMCs (1), our present studies demonstrate that loss of Atr expression affects VSMC migration and orientation, but not growth; thus Atrs may participate in part, but not all, of the Fat1-mediated effects on VSMC activities. Interestingly, these results are consistent with descriptions of

Atr mutant phenotypes in *Drosophila*, which show defects in cell fate and patterning similar to Fat mutants but lack the tumor suppressor phenotype found in the latter (5). Although Atrophin regulates planar cell polarity in *Drosophila*, and Atr2L is required for proper formation of critical signaling centers in early vertebrate development, a specific effect of Atrs on cellular migration and/or orientation has not been reported previously.

Re-expression of fetal developmental genes in the setting of vascular injury is well known (35). Distinct regulation of Atr isoforms after injury suggests, however, a level of control of Atr activity that has evolved since the divergence of metazoan lineages leading to insects and vertebrates. One possible explanation for the distinct effects of different Atr isoforms on migration and orientation is that although Atr2L acts to limit migration and orientation, this effect is opposed by the short isoforms, Atr1 and Atr2S. The short isoforms lack the N-terminal domains that interact with histone deacetylases (21, 22, 32) and conceivably could interfere with gene repression mediated by long forms of Atr (19, 36). Such a model is compelling in part given the preferential induction of the short isoforms by promigratory growth factors and by arterial injury (Fig. 1); in these settings, inhibition of Atr2L-mediated gene repression by induction of the short isoforms might allow transcriptional reprogramming of VSMCs to support a more migratory phenotype. In addition, we surmise that the (nonessential) short isoforms may have evolved to add a higher layer of regulation to the (essential) evolutionarily conserved long form of Atr. This also raises the question of whether analogous but necessarily distinct mechanisms of Atrophin regulation exist in *Drosophila*, which have only a single long Atrophin isoform.

We developed evidence along several lines that support the validity and significance of the Atr-Fat1 interaction; both proteins 1) show a similar pattern of regulation after vascular injury, which suggests a shared biological function, 2) colocalize within cells, 3) coimmunoprecipitate at endogenous levels of expression, and 4) depend on discrete sequences for their physical interaction, which argues against nonspecificity of the interaction. In addition, we found that enhanced VSMC migration mediated by Atr2L knockdown requires Fat1 expression. The mechanism underlying the opposing effects of Fat1 and Atr2L on migration is not yet clear. As discussed above, it may be that Atr2L, acting as a transcriptional repressor, controls expression of gene products directly involved in cellular migration as promoted by Fat1; by antagonizing Atr2L-mediated gene repression, the short Atr isoforms also enhance migration. Because Fat1 and Atrs interact at multiple cellular locations, alternative mechanisms must also be considered. For example, it is possible that Fat1-Atr1 or -Atr2S interactions at or near the cell surface could modify interactions of the $Fat1_{IC}$ domain with Ena/VASP proteins (13, 14), thereby promoting migration via effects on actin cytoskeletal remodeling; alternatively, $Fat1_{IC}$ domain in the cell nucleus (1, 24, 37) interacting with Atrs could affect Atr-mediated transcriptional activities at migration-related target genes. Future studies will address the precise mechanistic link between Fat1-Atr interactions and effects on VSMC activities and determine the significance of these interactions for VSMC migration and vascular disease.

Acknowledgments—We thank Nick Baker and Hanh Nguyen for critical reading of the manuscript.

REFERENCES

1. Hou, R., Liu, L., Anees, S., Hiroyasu, S., and Sibinga, N. E. S. (2006) *J. Cell Biol.* **173,** 417–429
2. Tanoue, T., and Takeichi, M. (2005) *J. Cell Sci.* **118,** 2347–2353
3. Halbleib, J. M., and Nelson, W. J. (2006) *Genes Dev.* **20,** 3199–3214
4. Bryant, P. J., Huettner, B., Held, L. I., Jr., Ryerse, J., and Szidonya, J. (1988) *Dev. Biol.* **129,** 541–554
5. Fanto, M., Clayton, L., Meredith, J., Hardiman, K., Charroux, B., Kerridge, S., and McNeill, H. (2003) *Development* **130,** 763–774
6. Cho, E., Feng, Y., Rauskolb, C., Maitra, S., Fehon, R., and Irvine, K. D. (2006) *Nat. Genet.* **38,** 1142–1150
7. Silva, E., Tsatskis, Y., Gardano, L., Tapon, N., and McNeill, H. (2006) *Curr. Biol.* **16,** 2081–2089
8. Thompson, B. J., and Cohen, S. M. (2006) *Cell* **126,** 767–774
9. Willecke, M., Hamaratoglu, F., Kango-Singh, M., Udan, R., Chen, C. L., Tao, C., Zhang, X., and Halder, G. (2006) *Curr. Biol.* **16,** 2090–2100
10. Tyler, D. M., and Baker, N. E. (2007) *Dev. Biol.* **305,** 187–201
11. Castillejo-Lopez, C., Arias, W. M., and Baumgartner, S. (2004) *J. Biol. Chem.* **279,** 24034–24043
12. Ciani, L., Patel, A., Allen, N. D., and ffrench-Constant, C. (2003) *Mol. Cell. Biol.* **23,** 3575–3582
13. Tanoue, T., and Takeichi, M. (2004) *J. Cell Biol.* **165,** 517–528
14. Moeller, M. J., Soofi, A., Braun, G. S., Li, X., Watzl, C., Kriz, W., and Holzman, L. B. (2004) *EMBO J.* **23,** 3769–3779
15. Nakaya, K., Yamagata, H. D., Arita, N., Nakashiro, K. I., Nose, M., Miki, T., and Hamakawa, H. (2007) *Oncogene* **26,** 5300–5308
16. Matsui, S., Utani, A., Takahashi, K., Mukoyama, Y., Miyachi, Y., and Matsuyoshi, N. (2008) *J. Dermatol. Sci.* **51,** 207–210
17. Saburi, S., Hester, I., Fischer, E., Pontoglio, M., Eremina, V., Gessler, M., Quaggin, S. E., Harrison, R., Mount, R., and McNeill, H. (2008) *Nat. Genet.* **40,** 1010–1015
18. Zhang, S., Xu, L., Lee, J., and Xu, T. (2002) *Cell* **108,** 45–56
19. Shen, Y., Lee, G., Choe, Y., Zoltewicz, J. S., and Peterson, A. S. (2007) *J. Biol. Chem.* **282,** 5037–5044
20. Zoltewicz, J. S., Stewart, N. J., Leung, R., and Peterson, A. S. (2004) *Development* **131,** 3–14
21. Wang, L., Rajan, H., Pitman, J. L., McKeown, M., and Tsai, C. C. (2006) *Genes Dev.* **20,** 525–530
22. Plaster, N., Sonntag, C., Schilling, T. F., and Hammerschmidt, M. (2007) *Dev. Dyn.* **236,** 1891–1904
23. Bustin, S. A. (2000) *J. Mol. Endocrinol.* **25,** 169–193
24. Braun, G. S., Kretzler, M., Heider, T., Floege, J., Holzman, L. B., Kriz, W., and Moeller, M. J. (2007) *J. Biol. Chem.* **282,** 22823–22833
25. Savani, R. C., Wang, C., Yang, B., Zhang, S., Kinsella, M. G., Wight, T. N., Stern, R., Nance, D. M., and Turley, E. A. (1995) *J. Clin. Invest.* **95,** 1158–1168
26. Mercure, M. Z., Ginnan, R. P. D., and Singer, H. A. (2008) *Am. J. Physiol.* **294,** C1465–C1475
27. Nagafuchi, S., Yanagisawa, H., Ohsaki, E., Shirayama, T., Tadokoro, K., Inoue, T., and Yamada, M. (1994) *Nat. Genet.* **8,** 177–182
28. Khan, F. A., Margolis, R. L., Loev, S. L., Sharp, A. H., Li, S. H., and Ross, C. A. (1996) *Neurobiol. Dis.* **3,** 121–128
29. Riley, B. E., and Orr, H. T. (2006) *Genes Dev.* **20,** 2183–2192
30. Erkner, A., Roure, A., Charroux, B., Delaage, M., Holway, N., Core, N., Vola, C., Angelats, C., Pages, F., Fasano, L., and Kerridge, S. (2002) *Development* **129,** 1119–1129
31. Wood, J. D., Nucifora, F. C., Jr., Duan, K., Zhang, C., Wang, J., Kim, Y., Schilling, G., Sacchi, N., Liu, J. M., and Ross, C. A. (2000) *J. Cell Biol.* **150,** 939–948

32. Zhang, C. L., Zou, Y., Yu, R. T., Gage, F. H., and Evans, R. M. (2006) *Genes Dev.* **20,** 1308–1320
33. Waerner, T., Gardellin, P., Pfizenmaier, K., Weith, A., and Kraut, N. (2001) *Cell Growth Differ.* **12,** 201–210
34. Karres, J. S., Hilgers, V., Carrera, I., Treisman, J., and Cohen, S. M. (2007) *Cell* **131,** 136–145
35. Majesky, M., Giachelli, C., Reidy, M., and Schwartz, S. (1992) *Circ. Res.* **71,** 759–768
36. Charroux, B., Freeman, M., Kerridge, S., and Baonza, A. (2006) *Dev. Biol.* **291,** 278–290
37. Magg, T., Schreiner, D., Solis, G. P., Bade, E. G., and Hofer, H. W. (2005) *Exp. Cell Res.* **307,** 100–108